COPY NO. 7
RM E9E16

NACA RM E9E16

NACA

RESEARCH MEMORANDUM

EFFECT OF TEMPERATURE ON PERFORMANCE OF SEVERAL EJECTOR CONFIGURATIONS

By H. D. Wilsted, S. C. Huddleston
and C. W. Ellis

Lewis Flight Propulsion Laboratory
Cleveland, Ohio

NATIONAL ADVISORY COMMITTEE
FOR AERONAUTICS

WASHINGTON
June 13, 1949

NACA RM E9E16

NATIONAL ADVISORY COMMITTEE FOR AERONAUTICS

RESEARCH MEMORANDUM

EFFECT OF TEMPERATURE ON PERFORMANCE OF SEVERAL EJECTOR CONFIGURATIONS

By H. D. Wilsted, S. C. Huddleston
and C. W. Ellis

SUMMARY

An investigation was made to determine the effect of the primary-jet temperature on the performance of several ejector configurations. The performance of ejectors expressed in terms of the ratio of weight of secondary air flow to primary air flow (weight-flow ratio) was found to be affected by temperature in two ways. Increasing the temperature of the primary jet decreases the primary weight flow with the result that the weight-flow ratio tends to increase. Addition of heat to the primary jet, however, increases the pressure in the plane of discharge of the primary nozzle with the result that less secondary weight flow is induced and the weight flow ratio tends to decrease. The ejector performance then depends upon the relative magnitude of the two effects and these depend upon the ejector configuration being used.

In general, for the ejectors with short straight mixing lengths and short spacings, the weight-flow ratio varies directly as the square root of the ratio of the total primary temperature to the total secondary temperature. For the ejectors with longer lengths and spacings, which pump greater weight flows through the secondary annulus, however, the pressure increase in the plane of the primary-nozzle exit decreases the secondary weight flow so much that the temperature-ratio correction factor does not completely describe the temperature effect on ejector performance.

INTRODUCTION

With the advent of high-power-output turbojet and turbine-propeller power-plant installations in aircraft, increased amounts of cooling air are required for turbine disks, turbine blades, bearings, the tail pipe, and the fuselage-structure. Under cruising flight conditions, the cooling-air requirements can often be supplied by ram air. For ground operation and climb and for installations utilizing tail-pipe burning for thrust augmentation, a means

of supplying additional air for cooling must be provided. One of the most practical pumps for this type of service is the jet-actuated ejector, which is of simple construction, adds little weight, and generally achieves pumping with no loss to the primary stream. The ejector has also been proposed as a pump for removing boundary-layer air from aircraft-wing, control, and fuselage surfaces.

As part of a program to study the theoretical and practical aspects of air ejectors for application to jet-type power plants, an investigation was conducted at the NACA Lewis laboratory to determine the degree of correlation that can be obtained with data from models with unheated jets and from ejectors mounted on a full-scale turbojet engine. The primary-jet-nozzle portion of the ejector was first investigated to supply design information. Flow coefficients and velocity coefficients for a wide range of conical-type jet nozzles are reported in reference 1. Ejector data from an investigation of model conical-mixing-section type ejectors have been published in reference 2. These ejectors had a primary-jet exit diameter of 4.00 inches. The ratios of mixing-cone exit diameter to primary-jet exit diameter investigated were 1.00, 1.10, and 1.21. These ejectors induced secondary air flows in a range sufficient for most turbojet cooling requirements.

An analytical and experimental investigation of the effect of primary-jet temperature on ejector performance is presented herein. Data from model ejectors having a 4.00-inch-diameter primary jet nozzle and an unheated primary-jet air supply are compared with data obtained from an ejector installation on a turbojet engine having a 12.40-inch-diameter primary jet nozzle in which the primary-jet air-supply temperature varied from approximately 800° to 1200° F.

Higher-capacity ejectors with straight mixing sections have been included in this investigation in addition to the conical-mixing-section type ejectors because of possible application to boundary-layer removal.

SYMBOLS

The ejector dimensions are shown in the following sketch:

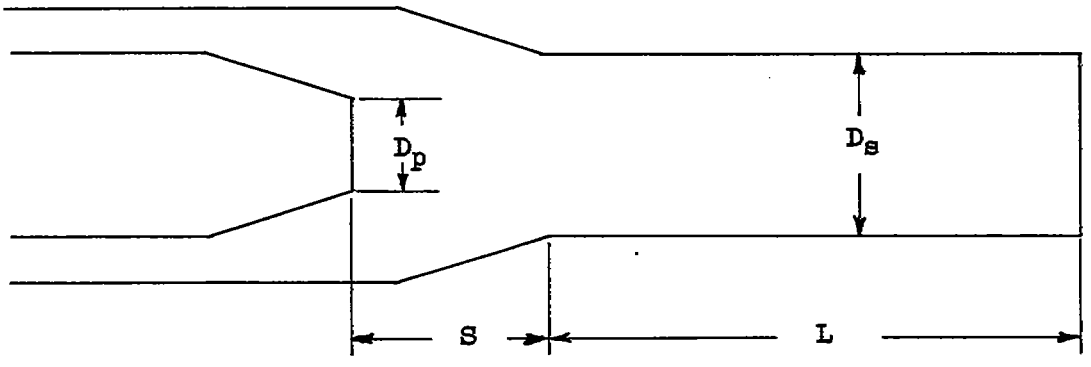

The following symbols are used in this report:

A cross-sectional area

D diameter

F pressure factor

g acceleration due to gravity

L length of straight mixing section

P total pressure

p static pressure

R gas constant

S spacing, distance from primary-nozzle exit to conical-mixing-section exit

T total temperature

W weight flow

γ ratio of specific heats

Subscripts:

c ejector with cold primary stream

h ejector with hot primary stream

p primary stream of ejector

s secondary stream of ejector

0 ambient

1 total-temperature and total-pressure stations upstream of mixing section

2 primary-jet-nozzle exit

3 secondary-jet-nozzle exit

ANALYSIS

One-Dimensional-Flow Equations

An examination of the factors affecting the flow within the ejector is presented. The primary fluid expands through the primary nozzle to a high velocity in the mixing section and diffuses until ambient pressure is reached at the mixing-section exit. (See following sketch of ejector nozzle.) Secondary flow is induced by the pressure difference between stations 2 and 1 in the secondary channel.

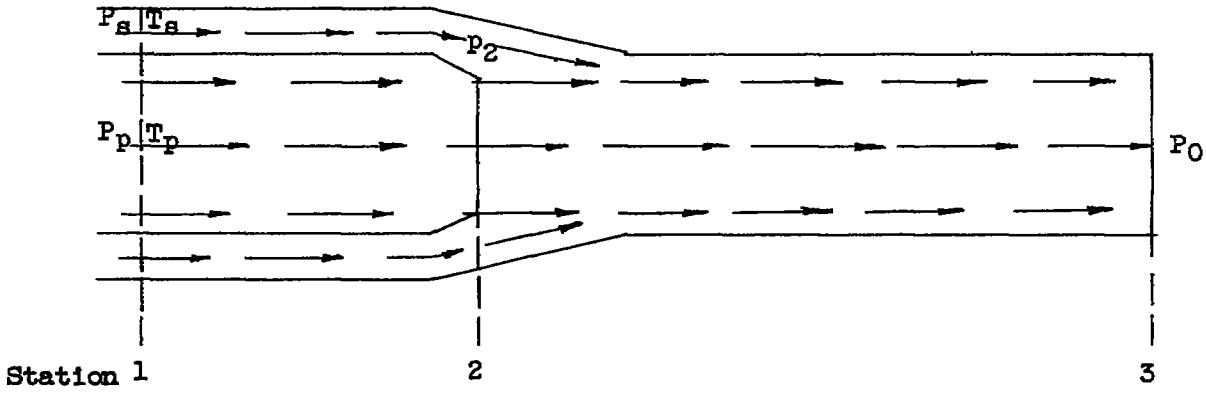

The fundamental equation for weight flow in a channel of varying cross section, based on one-dimensional compressible-flow theory is

$$W = A_2 \frac{P_1}{\sqrt{RT_1}} \sqrt{2g \frac{\gamma}{\gamma-1} \left[\left(\frac{p_2}{P_1}\right)^{\frac{2}{\gamma}} - \left(\frac{p_2}{P_1}\right)^{\frac{\gamma+1}{\gamma}} \right]} \qquad (1)$$

Ejector performance, expressed in terms of the ratio of weight flow through the secondary system to weight flow through the primary system, can be obtained by applying equation (1) to the primary and secondary systems. This expression is:

$$\frac{W_s}{W_p} = \left(\frac{A_{s,2}}{A_{p,2}}\right) \left(\frac{P_{s,1}}{P_{p,1}}\right) \sqrt{\frac{T_{s,1}}{T_{p,1}}} \sqrt{\frac{\left(\frac{\gamma}{\gamma-1}\right)_s \left[\left(\frac{p_2}{P_1}\right)^{\frac{2}{\gamma}} - \left(\frac{p_2}{P_1}\right)^{\frac{\gamma+1}{\gamma}} \right]_s}{\left(\frac{\gamma}{\gamma-1}\right)_p \left[\left(\frac{p_2}{P_1}\right)^{\frac{2}{\gamma}} - \left(\frac{p_2}{P_1}\right)^{\frac{\gamma+1}{\gamma}} \right]_p}} \qquad (2)$$

The ratio of the performance of a hot ejector to that of a cold ejector can be expressed by applying equation (2) to a hot-ejector system and a cold-ejector system.

$$\frac{\left(\frac{W_s}{W_p}\right)_h}{\left(\frac{W_s}{W_p}\right)_c} = \frac{\left(\frac{A_{s,2}}{A_{p,2}}\right)_h}{\left(\frac{A_{s,2}}{A_{p,2}}\right)_c} \frac{\left(\frac{P_{s,1}}{P_{p,1}}\right)_h}{\left(\frac{P_{s,1}}{P_{p,1}}\right)_c} \frac{\sqrt{\left(\frac{T_{p,1}}{T_{s,1}}\right)_h}}{\sqrt{\left(\frac{T_{p,1}}{T_{s,1}}\right)_c}} \sqrt{\frac{\left\{ \frac{\left(\frac{\gamma}{\gamma-1}\right)_s \left[\left(\frac{p_2}{P_1}\right)^{\frac{2}{\gamma}} - \left(\frac{p_2}{P_1}\right)^{\frac{\gamma+1}{\gamma}} \right]_s}{\left(\frac{\gamma}{\gamma-1}\right)_p \left[\left(\frac{p_2}{P_1}\right)^{\frac{2}{\gamma}} - \left(\frac{p_2}{P_1}\right)^{\frac{\gamma+1}{\gamma}} \right]_p} \right\}_h}{\left\{ \frac{\left(\frac{\gamma}{\gamma-1}\right)_s \left[\left(\frac{p_2}{P_1}\right)^{\frac{2}{\gamma}} - \left(\frac{p_2}{P_1}\right)^{\frac{\gamma+1}{\gamma}} \right]_s}{\left(\frac{\gamma}{\gamma-1}\right)_p \left[\left(\frac{p_2}{P_1}\right)^{\frac{2}{\gamma}} - \left(\frac{p_2}{P_1}\right)^{\frac{\gamma+1}{\gamma}} \right]_p} \right\}_c}} \qquad (3)$$

In order to simplify the equation, the last factor on the right side of equation (3) is defined as the pressure factor F and equation (4) becomes

$$\frac{\left(\frac{W_s}{W_p}\right)_h}{\left(\frac{W_s}{W_p}\right)_c} = \frac{\left(\frac{A_{s,2}}{A_{p,2}}\right)_h}{\left(\frac{A_{s,2}}{A_{p,2}}\right)_c} \frac{\left(\frac{P_{s,1}}{P_{p,1}}\right)_h}{\left(\frac{P_{s,1}}{P_{p,1}}\right)_c} \sqrt{\frac{\left(\frac{T_{p,1}}{T_{s,1}}\right)_h}{\left(\frac{T_{p,1}}{T_{s,1}}\right)_c}} \quad F \qquad (4)$$

Effect of Flow Parameters on Weight-Flow Ratio

Area and upstream-pressure parameter. - When equation (4) is applied to compare the performance at different temperatures of geometrically similar ejectors or of the same ejector operated at different temperatures, the area-ratio factor of equation (4) equals 1.0 when thermal expansion is neglected, and therefore this term can be dropped. Also, because comparison is made at the same operating conditions, the ratio of the total-pressure factors is equal to 1.0 and can be dropped.

Temperature parameter. - The temperature-ratio factor deviates considerably from unity, depending directly upon the square root of the temperature ratio of the hot ejector. When the ejector is used on a turbojet engine, the ratio of primary-air temperature to secondary-air temperature is of the order of 3, which gives a value of about 1.73 for the temperature-ratio factor. This factor by itself indicates that the weight-flow ratio for the hot ejector is 73 percent greater than that for the cold ejector when the hot ejector is operating with a temperature ratio of 3. The increase in weight-flow ratio of the hot ejector is due to the reduced weight flow of the hot primary fluid, which varies as the inverse of the square root of the temperature.

Exit pressure and specific-heat-ratio parameter. - The last factor in equation (3) is a function of the ratio of specific heats and the pressure ratio between stations 1 and 2 for each of the four flow systems. The ratio of specific heats is a function of temperature and fuel-air ratio. The total pressures at station 1 for the primary and secondary stream are independent variables and would be duplicated in the hot- and cold-ejector systems. The remaining factor to be considered is the pressure in the plane of the exit of the primary nozzle p_2.

In order to evaluate the effect of temperature on p_2, an analysis was made using the charts and the method outlined in reference 3. Steady one-dimensional compressible flow and complete mixing of the primary and secondary streams are assumed in this analysis. The results of the calculations are shown in figure 1. Pressure p_2 is plotted against primary total-to-ambient pressure ratio for an ejector with a diameter ratio of 2.1. Curves are shown for secondary total-to-ambient pressure ratios of 1.0 and 0.95 at primary-air temperatures of 1660° and 540° R. These curves indicate that the effect of increasing primary air temperature is to increase p_2. The pressure difference $p_{2,h} - p_{2,c}$ increases with increasing primary pressure ratio and decreases with decreasing secondary pressure ratio. Because $p_{2,h}$ is higher than $p_{2,c}$, less secondary weight flow is induced in the hot operated ejector.

The preceding analysis, with complete mixing assumed, yields the maximum theoretical value of $p_{2,h} - p_{2,c}$ that would exist between hot and cold operated ejectors. Actual ejector configurations would yield less difference in p_2, the amount varying with the ejector configuration considered. The effect on performance of small differences in $p_{2,h}$ and $p_{2,c}$ can be seen by considering the pressure factor F.

A plot of F against $p_{2,h}$ is shown in figure 2. The pressure $p_{2,c}$ is held constant at 2000 pounds per square foot, whereas $p_{2,h}$ is varied. Curves I and II are for a secondary pressure of 2020 pounds per square foot and for primary total pressures of 3175 and 5080 pounds per square foot, respectively. Curve III is for a primary pressure of 3175 pounds per square foot and a secondary pressure of 2005 pounds per square foot. The three curves indicate that F does not vary greatly with changes in primary pressure but does vary considerably with secondary pressure.

The most significant fact brought out in figure 2 is the small difference between $p_{2,h}$ and $p_{2,c}$ required to make F an important factor in the comparison of hot and cold-ejector data. For instance, for operating conditions satisfied by curve III, a difference between $p_{2,h}$ and $p_{2,c}$ of 3 pounds per square foot gives a value of F of 0.65, and therefore $W_{s,h}$ would be 35 percent less than $W_{s,c}$. The curves of figure 2 are calculated curves

derived from assumed operating conditions and no methods other than experimental have so far been developed for determining at what points on the curve actual ejector configurations will be operating.

It seems reasonable to assume that ejector configurations that pump the greatest amount of secondary weight flow for a particular diameter ratio are the configurations in which complete mixing of the primary and secondary streams is most nearly achieved. These configurations are: (1) those having the straight mixing-section length that pumps the greatest amount of secondary air for a particular spacing and diameter ratio, and (2) those with no straight mixing section having the spacing S that pumps the greatest amount of secondary air for each diameter ratio. These configurations would approach the ideal complete mixing to varying degrees and would also show the greatest difference between $p_{2,h}$ and $p_{2,c}$. The opposite extreme is those configurations of short length and spacing in which mixing is very incomplete and no difference exists between $p_{2,h}$ and $p_{2,c}$.

Summary of Analysis

Increasing the temperature of the primary jet affects the ejector performance: first by decreasing the weight flow of the primary stream, which tends to increase the weight-flow ratio of the ejector; second, by increasing the pressure that induces secondary flow so that secondary weight flow is decreased. The over-all effect for a particular temperature of the primary stream depends upon the relative magnitude of the two effects, which depends upon the ejector configuration being used.

APPARATUS AND PROCEDURE

In order to determine how the over-all temperature effect varies with various configurations, a selected group of ejectors were investigated when hot on a full-scale turbojet-engine setup and when cold on a model setup. It was recognized that flow similarity must be established between the model and full-scale setup in order to allow direct comparison of data. This requirement necessitates geometric similarity of the ejectors and equivalent Reynolds numbers and Mach numbers. Geometric similarity was obtained by comparing model and full-scale data of similar configurations. A curve of Reynolds number is presented in reference 1 plotted against pressure ratio for a range of full-scale and model nozzle diameters covering the nozzles used in the

investigation reported herein. These curves show the Reynolds numbers of the model and full-scale primary nozzles to be of the same order of magnitude. Another curve in reference 1 shows that for equal primary-pressure ratios the difference in Mach numbers is small for the model and full-scale ejectors. Inasmuch as geometric similarity was obtained and Reynolds numbers and Mach numbers were duplicated with reasonable accuracy, the model and full-scale investigations are considered to be comparable for evaluating primary-temperature effects.

The cold-ejector investigations were conducted on the apparatus diagrammatically shown in figure 3. The high-velocity air of the primary jet discharges into the mixing sections and induces the flow of secondary air through the concentric secondary approach section. The primary and secondary systems are so separated as to permit measurement of the flow through each system and to control the pressure in each system independently. Air flow was measured by standard A.S.M.E. sharp-edged orifices. Temperatures were measured by bare iron-constantan thermocouples and a self-balancing potentiometer. The upstream instrumentation in the primary jet was located 4 jet-exit diameters upstream of the jet exit and consisted of one total-pressure tube and one thermocouple inserted into the stream one-third of the pipe diameter. The instrumentation for the secondary flow system (annular space between inner and outer piping) was located $4\frac{1}{4}$ primary-jet diameters from the primary jet-nozzle exit and consisted of two total-pressure tubes and two iron-constantan thermocouples.

The model air ejectors were made as large as possible (limited by air capacity available to setup) in order to minimize scale effects. The primary nozzle consisted of a 5.0-inch-inside-diameter approach pipe and a conical section with a 15° half-cone angle and an exit diameter of 4.0 inches. The conical mixing sections had a 15° half-cone angle and a 10.0-inch-diameter approach pipe. Various lengths of straight mixing section were added to the conical mixing section so that comparison with the full-scale data could be made.

The apparatus used for the full-scale ejector investigation is schematically shown in figure 4. The engine and the secondary-air system were mounted on a pendulum-type test stand in a sealed test cell. The combined primary- and secondary-air flow was measured by means of a standard A.S.M.E. nozzle. Atmospheric air was drawn through the nozzle into the sealed test cell. The secondary air flow was measured by two inlet-type orifices of the type described in reference 4. The secondary air flow was subtracted from the

combined flow to obtain the primary-jet air flow. The fuel flow was measured by rotameters and was added to the air flow to give the total primary weight flow. The instruments located upstream of the primary jet nozzle consisted of four bare chromel-alumel thermocouples and four total-pressure tubes. The instrumentation for the secondary-air-flow system consisted of four total-pressure tubes and four bare chromel-alumel thermocouples located at equal distances on the periphery of the mixing-tube cone, 8 inches from the face of the pressure-equalization chamber. The pressure tubes were located in the center of the flow annulus and the thermocouples were located in the center of each of four equal flow areas

The investigation was conducted by operating each of the models investigated over a range of primary-nozzle pressure ratios while holding the secondary-air pressure at the upstream station at a constant value. This procedure was repeated for two additional secondary pressures. The pressures in the primary and secondary systems were independently regulated by pneumatically operated butterfly valves. The air temperature in both the primary- and secondary-air streams was nearly constant at approximately 80° F.

The full-scale investigation was made in a similar manner. The primary-jet-nozzle supply pressure was changed by varying the engine rotor speed, and the secondary supply pressure at station l_s was regulated by hydraulically operated butterfly valves. The primary total temperatures varied from 800° to 1200° F, whereas the secondary total temperature varied from 70° to 100° F depending upon the secondary air flow being pumped.

The following configurations were investigated on both the model and the full-scale setup:

Diameter ratio D_s/D_p	Spacing S/D_p	Length-to-diameter ratio L/D_s
1.21	0.82	0.5
1.21	.82	1.0
1.21	.82	2.5
1.21	.82	4.5
1.21	1.64	0
1.10	1.1	0

These configurations were selected to show the temperature effect on ejector performance at various lengths of cylindrical mixing section as well as the performance of the zero-length conical-mixing-section type ejector at spacings that provide the maximum weight flow for diameter ratios of 1.21 and 1.10 as determined from reference 2.

RESULTS AND DISCUSSION

Data from the hot- and cold-ejector setups were compared for ejectors having the same geometric configurations. These data are shown in figures 5 to 7. In figure 5(a), the ratio of measured secondary weight flow to primary weight flow W_s/W_p is shown plotted against primary-nozzle pressure ratio (upstream total-to-ambient pressure ratio $P_{p,1}/p_0$). Three values of secondary total-to-ambient pressure ratio $P_{s,1}/p_0$ are indicated. At the high primary pressure ratios, the hot-ejector data show a weight-flow ratio from 50 to 80 percent higher than the cold-ejector data.

In the curves of figure 5(b), the hot-ejector data have been corrected by a temperature-ratio factor. If the factor F of equation (4) is 1.0,

$$(W_s/W_p)_{corr} = (W_s/W_p)_h \times \sqrt{(T_s/T_p)_h} \qquad (5)$$

Any disparity between $(W_s/W_p)_{corr}$ and $(W_s/W_p)_c$, other than that attributable to experimental error is considered to be caused by deviation of the factor F from unity. A comparison of the corrected hot-ejector data and the cold-ejector data is shown in figure 5(b). For this configuration, the factor F is evidently very close to 1.0 inasmuch as satisfactory agreement exists between the hot-ejector corrected data and cold-ejector data.

The corrected hot-ejector data are compared with the cold-ejector data for several configurations in figures 5(c) to 7. For the ejectors at a diameter ratio of 1.21 and short lengths, satisfactory agreement exists between the corrected hot-ejector and the cold-ejector data. As additional lengths of straight mixing section were added, however, the corrected hot-ejector and cold-ejector performance diverged, with the corrected hot-ejector data falling below the cold-ejector data. This effect is shown more clearly in

figure 6, which shows the effect of mixing length on the agreement between corrected hot-ejector and cold-ejector data. This figure is a cross plot of figure 5 at a primary pressure ratio $P_{p,1}/p_0$ of 1.50 and a secondary pressure ratio $P_{s,1}/p_0$ of 0.925. In addition, unpublished data for a cold ejector at zero length and a hot ejector at a length-to-diameter ratio of 0.1 have been added to the data reported herein to complete the curve of figure 6. Corrected weight-flow ratio $W_s/W_p\sqrt{T_s/T_p}$ is plotted against mixing-section length-to-diameter ratio L/D_s. At an L/D_s of 4.50, the corrected hot-ejector data are approximately 14 percent below that of the cold-ejector data. The dashed line is for cold-ejector data and the solid curve is for the corrected hot-ejector data.

For a diameter ratio of 1.21 and a spacing of 0.82, figure 6 indicates that for cold-ejector data a length-to-diameter ratio of approximately 4.25 pumps the greatest weight flow through the secondary nozzle. For the corrected hot-ejector data, this ratio for maximum pumping is reduced to approximately 2.75. The L/D for maximum weight-flow ratio is lower for the hot ejector, apparently because of greater friction losses in the higher velocity hot jet.

Data are shown in figure 7(a) for an ejector having a diameter ratio of 1.21 and a spacing of 1.64, which has a pumping capacity approximately equivalent to that of the spacing for maximum W_s/W_p, as indicated in reference 2. The cold-ejector performance was obtained by cross-plotting data from reference 2. These data also show that the corrected hot-ejector data fall below the cold-ejector data by about 15 percent at the high primary pressure ratios and a secondary pressure ratio of 0.925.

Data are shown in figure 7(b) for a diameter ratio of 1.10 and zero length for the spacing for maximum weight-flow ratio. Considerable difference again exists between corrected hot-ejector and cold-ejector data. At high primary pressures and a secondary pressure ratio of 0.925, the corrected hot-ejector data are as much as 35 percent below the cold-ejector data.

In general, for the lower-performance ejectors with short lengths and spacings, the factor F is so close to 1.0 that the temperature-ratio factor is sufficient to provide a satisfactory correlation factor for hot- and cold-ejector data. However with the higher-performance ejectors, (1) those that have lengths that

pump maximum weight flow for a particular spacing and diameter ratio and (2) those that have spacings that pump maximum weight flow for a particular diameter ratio and no length, the factor F becomes of considerable importance and cannot be neglected in correlating hot- and cold-ejector data.

Until further developments in mixing theory allow accurate determinations of the effect of various ejector configurations on p_2, a factor of safety must be allowed in selecting configurations to provide for the variation of the factor F. The upper limit of F is obtained by assuming p_2 equal in both hot and cold ejectors, which gives a value of F of approximately 1.0. For ejectors with zero spacing between the primary-nozzle exit and straight mixing section, reference 3 provides a method of determining $p_{2,h}$ and $p_{2,c}$ by analysis in which complete mixing is assumed.

CONCLUSIONS

The effect of primary-jet temperature on the performance of several ejector configurations was investigated in order to determine the effectiveness of predicting hot-ejector performance from cold-ejector data. Primary-jet temperature affects ejector performance in two ways. Increasing the temperature of the primary jet decreases the primary weight flow with the result that weight-flow ratio tends to increase. An increase in temperature of the primary fluid, however, increases the static pressure that induces secondary flow so that less weight flow is induced and the weight-flow ratio decreases. The resulting ejector performance depends upon the relative magnitude of the two effects and these depend upon the ejector configuration being used.

In general, for ejectors with short straight mixing lengths and short spacings, the second effect is negligible and the weight-flow ratio varies directly as the square root of the ratio of primary temperature to secondary temperature. With the higher-performance ejectors that have long lengths and spacings, however, the effect of the variation with temperature of pressure in the plane of the primary nozzle becomes important and cannot be neglected.

Lewis Flight Propulsion Laboratory,
National Advisory Committee for Aeronautics,
Cleveland, Ohio.

REFERENCES

1. Grey, R. E., and Wilsted, H. D.: Performance of Conical Jet Nozzles in Terms of Flow and Velocity Coefficients. NACA TN 1757, 1948.

2. Huddleston, S. C., Wilsted, H. D., and Ellis, C. W.: Performance of Several Air Ejectors with Conical Mixing Sections and Small Secondary Flow Rates. NACA RM E8D23, 1948.

3. Turner, L. Richard, Addie, Albert N., and Zimmerman, Richard H.: Charts for the Analysis of One-Dimensional Steady Compressible Flow. NACA TN 1419, 1948.

4. Ebaugh, N. C., and Whitfield, R.: The Intake Orifice and a Proposed Method for Testing Exhaust Fans. A.S.M.E. Trans., PTC-56-3, vol. 56, no. 12, Dec. 1945, pp. 903-911.

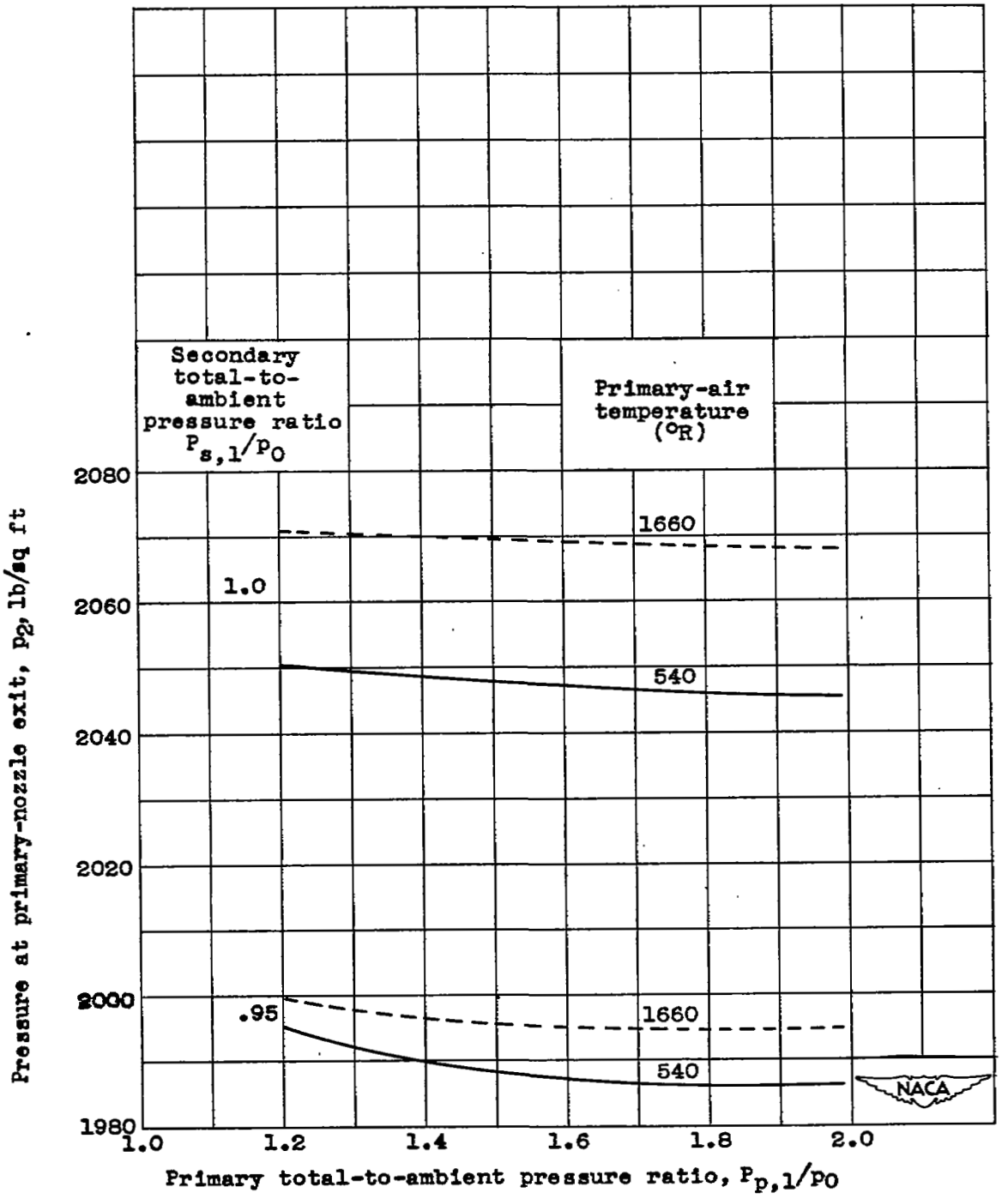

Figure 1. - Effect of temperature on pressure, inducing secondary weight flow of ejector with assumption of complete mixing (by method of reference 3). Diameter ratio D_s/D_p, 2.1; spacing S/D_p, 0.

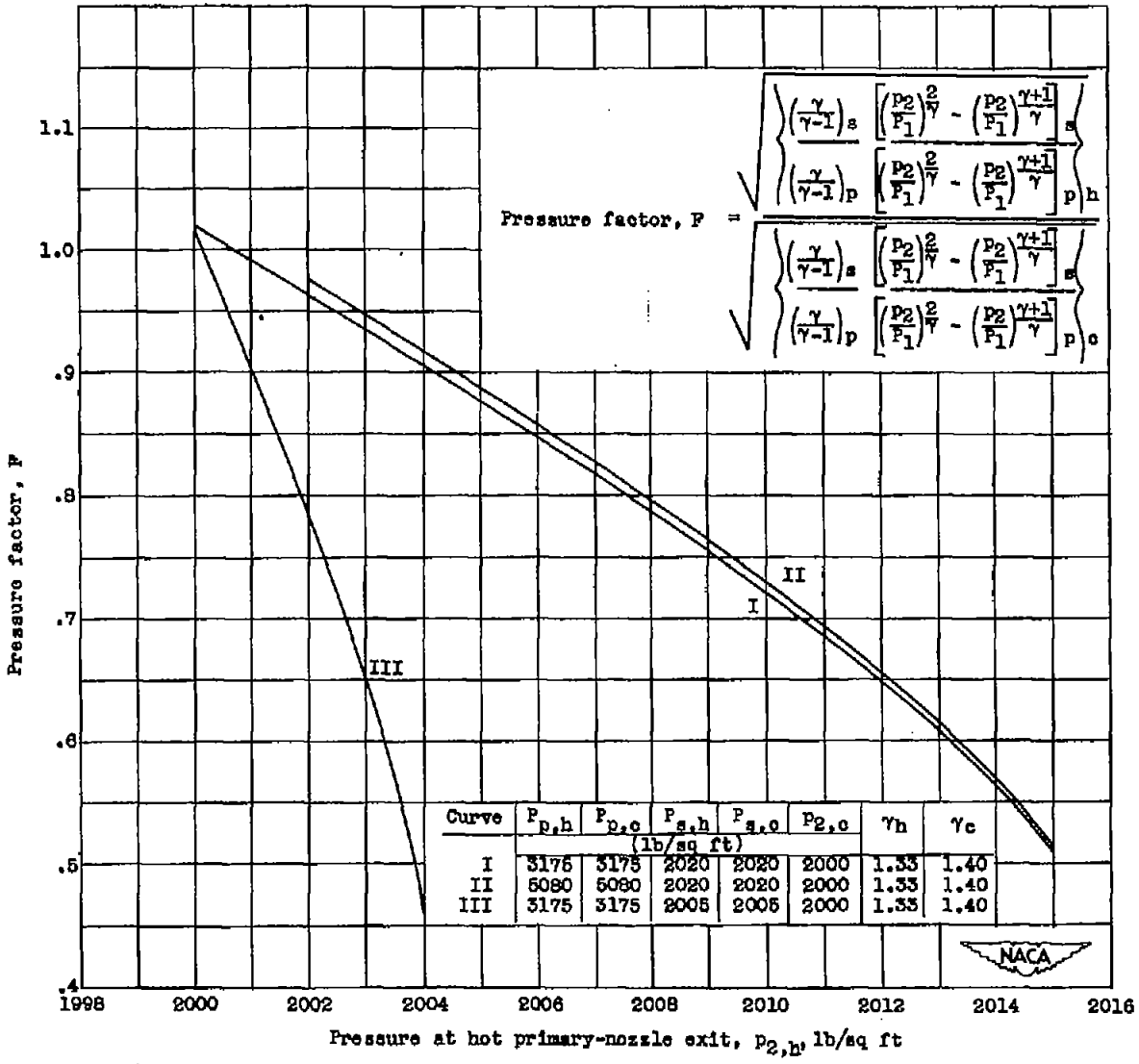

Curve	$P_{p,h}$	$P_{p,c}$	$P_{s,h}$	$P_{s,c}$	$P_{2,c}$	γ_h	γ_c
	(lb/sq ft)						
I	3175	3175	2020	2020	2000	1.33	1.40
II	5080	5080	2020	2020	2000	1.33	1.40
III	3175	3175	2005	2005	2000	1.33	1.40

Figure 2. - Pressure factor as affected by variation of $p_{2,h}$ from $p_{2,c}$.

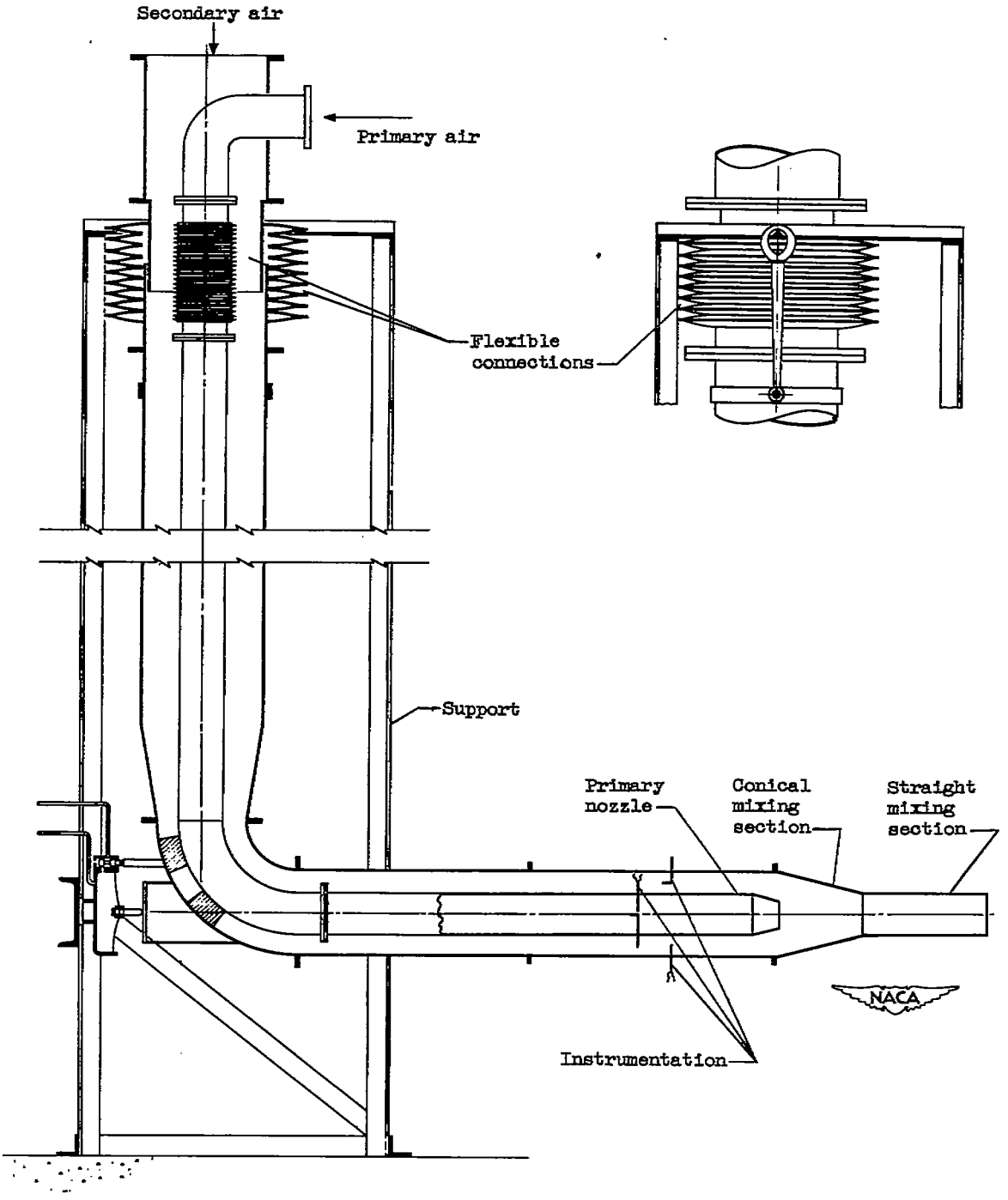

Figure 3. - Schematic diagram of model setup for cold-ejector investigation.

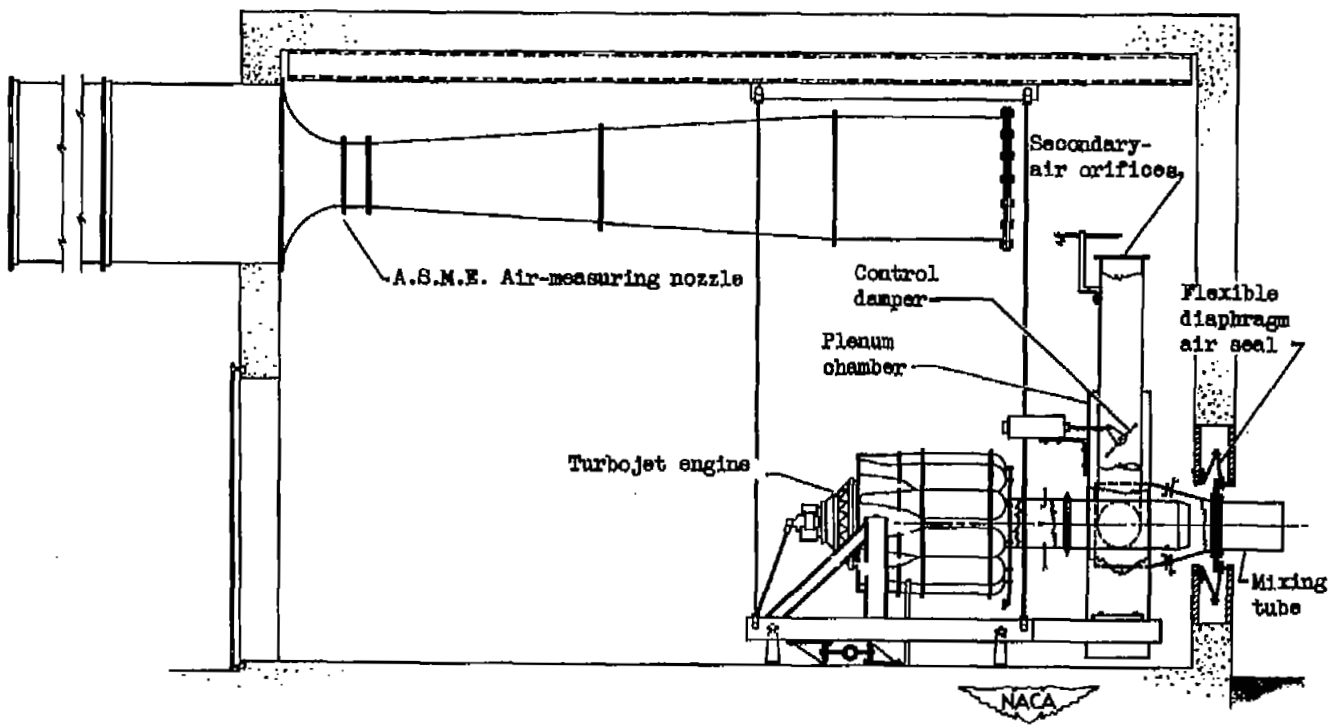

Figure 4. - Diagrammatic sketch of full-scale-ejector setup.

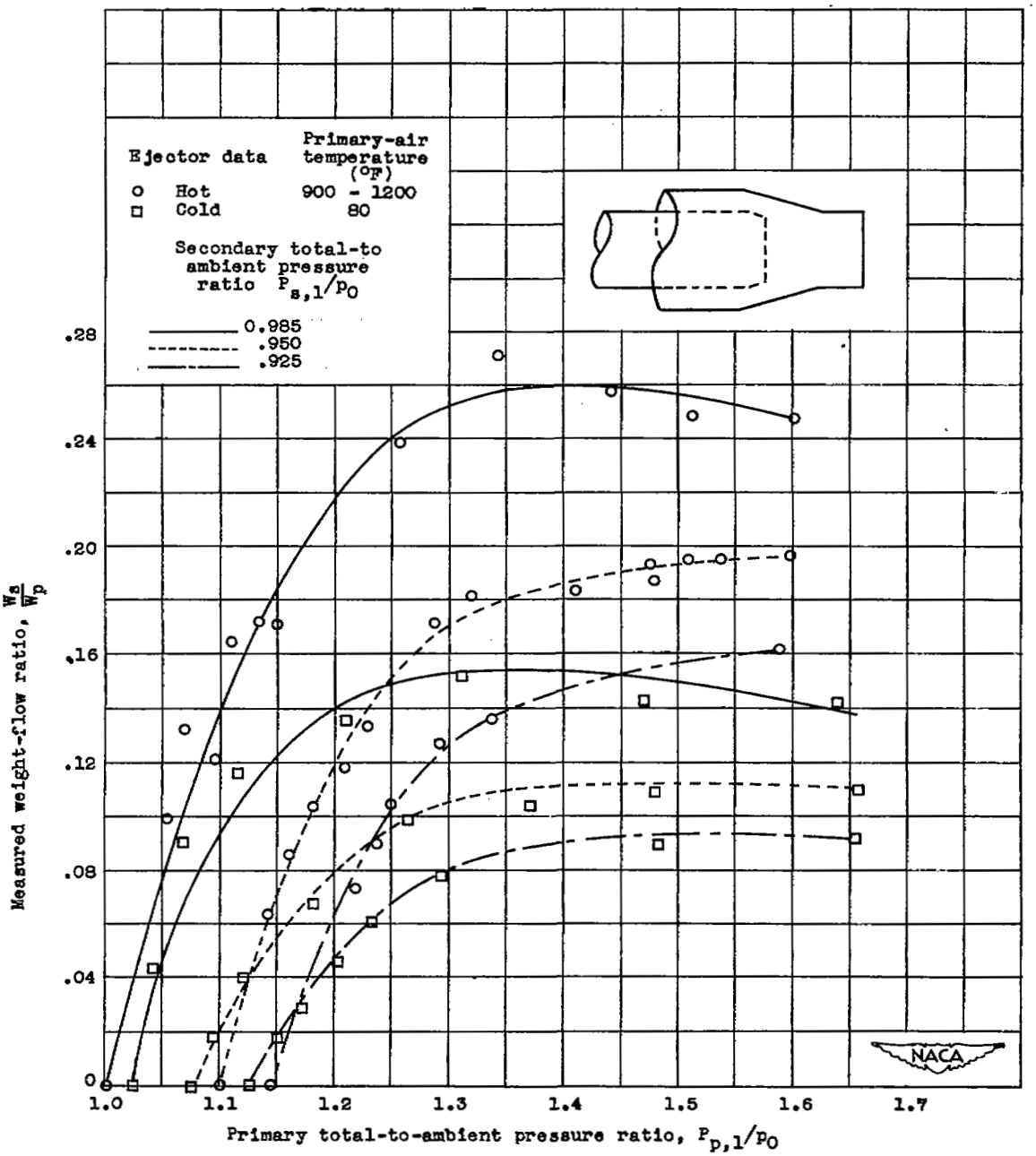

(a) Length-to-diameter ratio L/D_s, 0.50; uncorrected data.

Figure 5. - Comparison of hot- and cold-ejector performance for various length-to-diameter ratios. Diameter ratio D_s/D_p, 1.21; spacing S/D_p, 0.82.

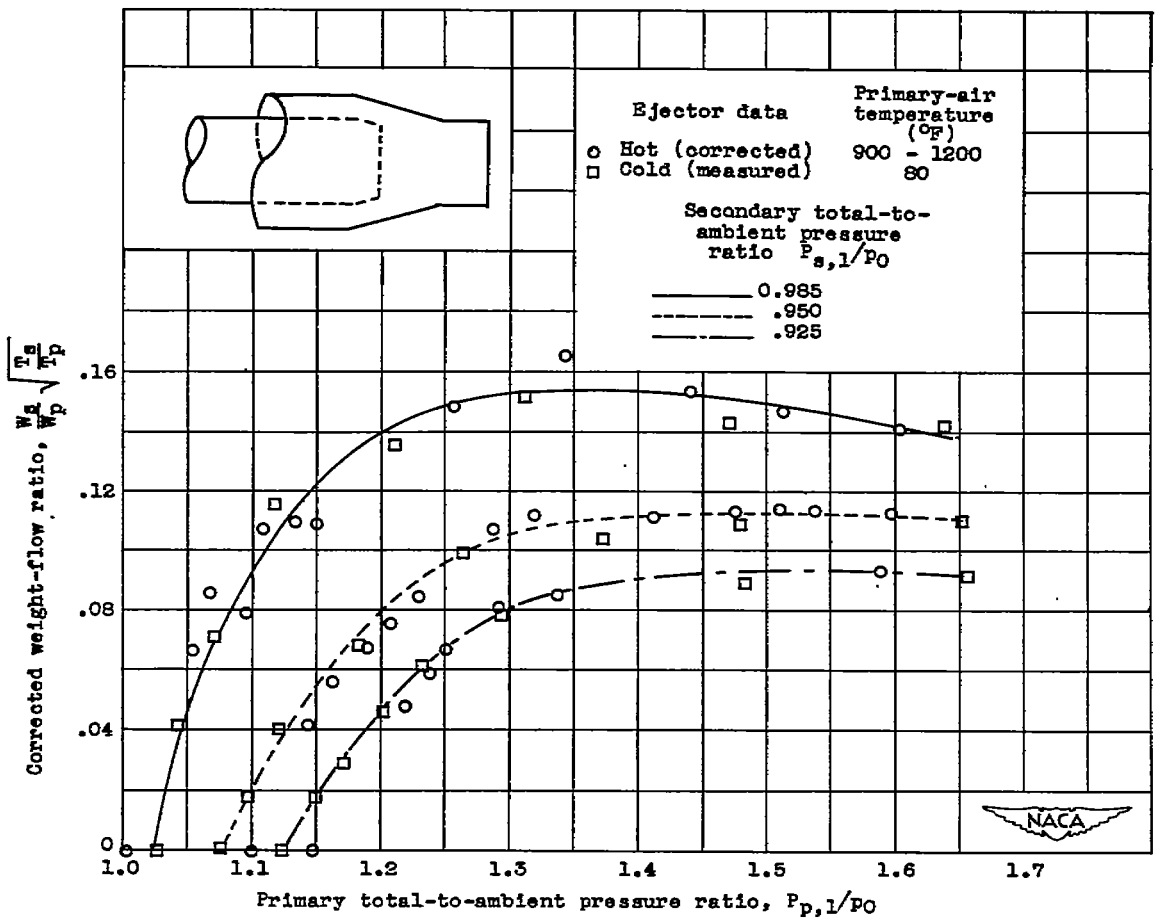

(b) Length-to-diameter ratio L/D_s, 0.50; corrected data.

Figure 5. - Continued. Comparison of hot- and cold-ejector performance for various length-to-diameter ratios. Diameter ratio D_s/D_p, 1.21; spacing S/D_p, 0.82.

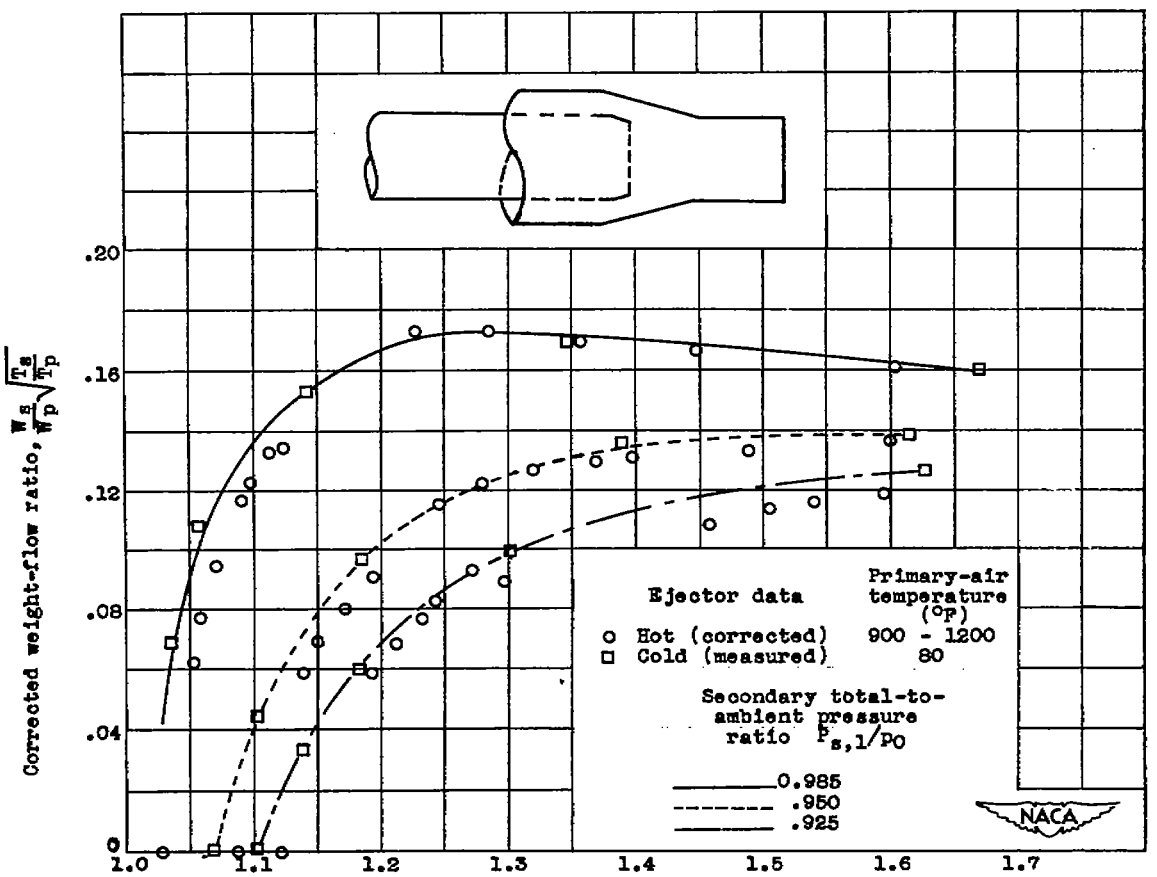

(c) Length-to-diameter ratio L/D_s, 1.00; corrected data.

Figure 5. - Continued. Comparison of hot- and cold-ejector performance for various length-to-diameter ratios. Diameter ratio D_s/D_p, 1.21; spacing S/D_p, 0.82.

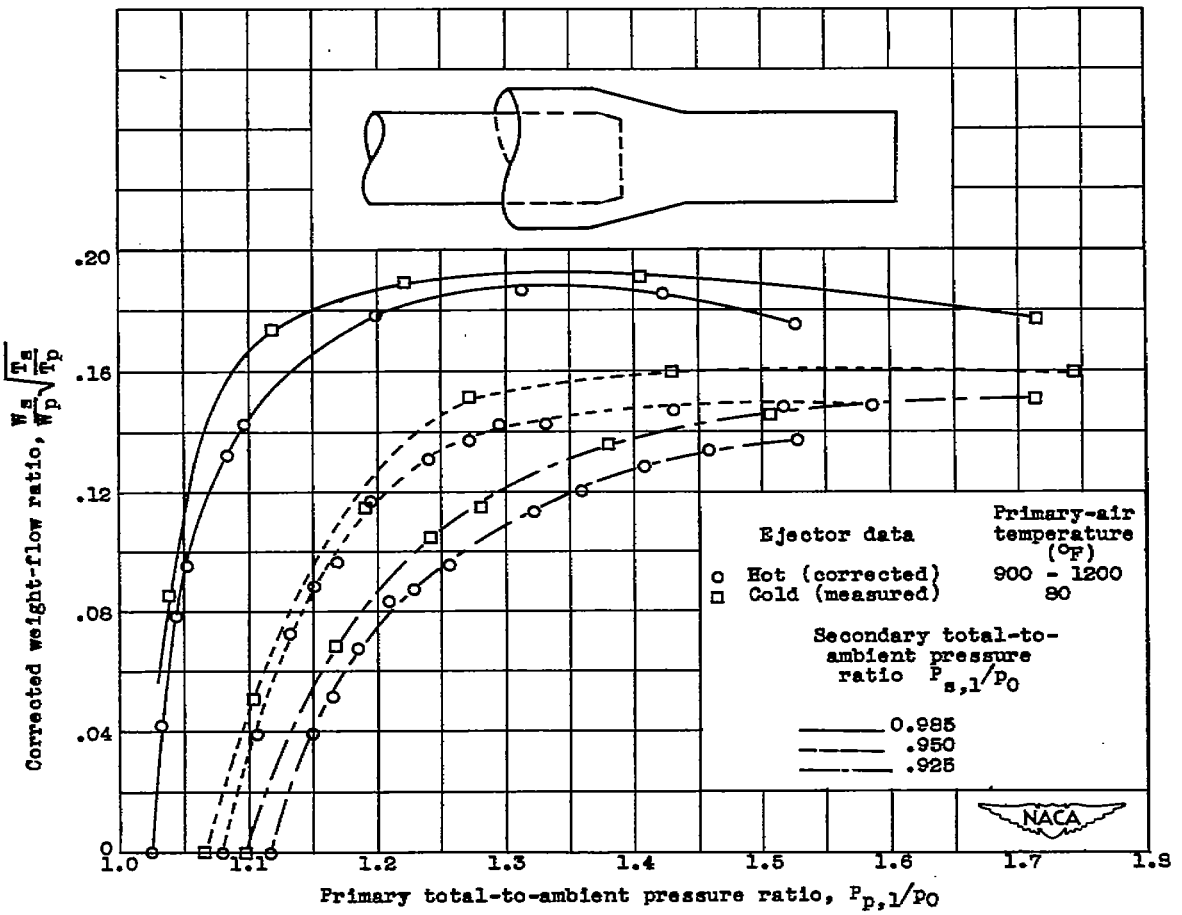

(d) Length-to-diameter ratio L/D_s, 2.50; corrected data.

Figure 5. - Continued. Comparison of hot- and cold-ejector performance for various length-to-diameter ratios. Diameter ratio D_s/D_p, 1.21; spacing S/D_p, 0.82.

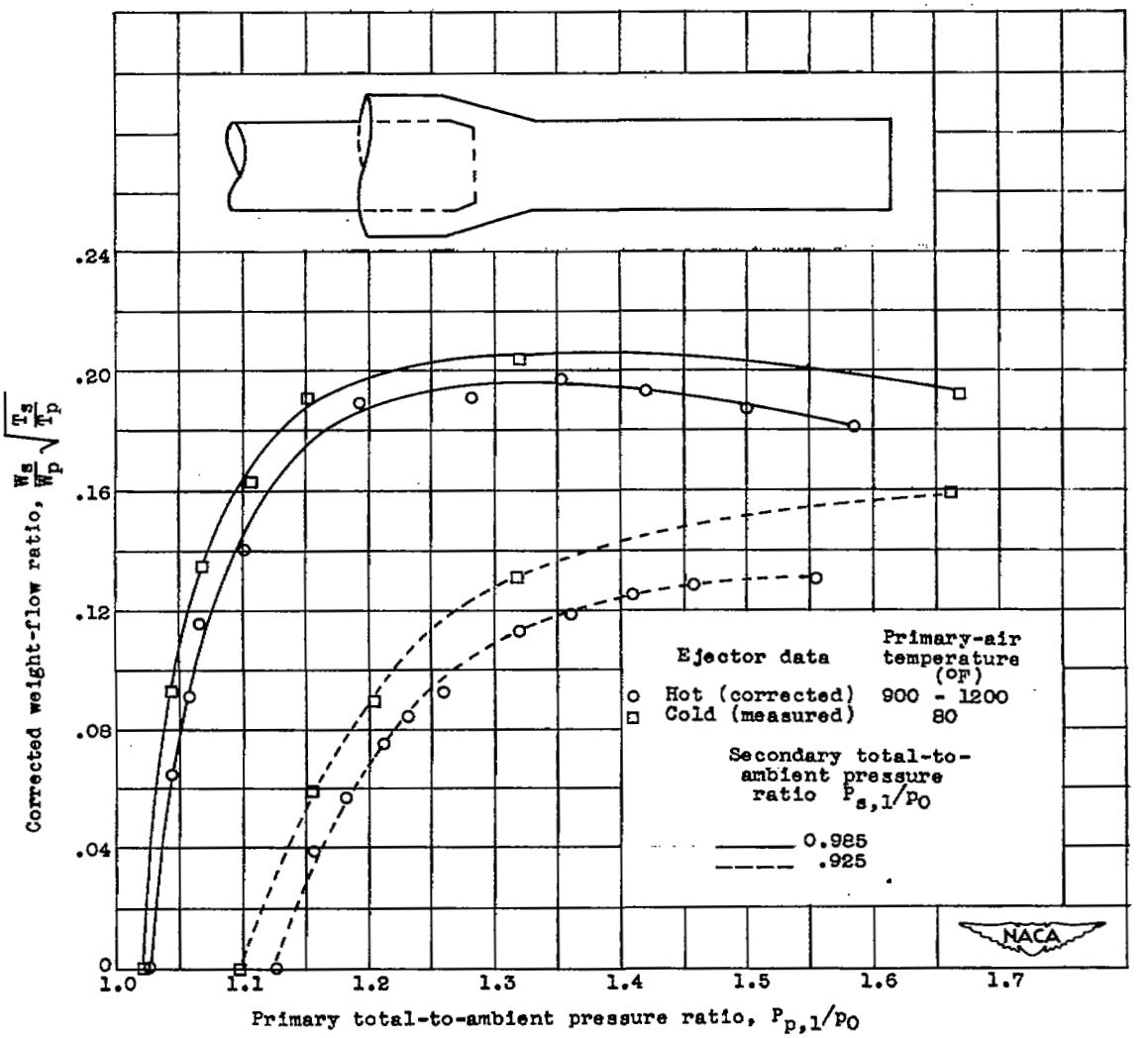

(e) Length-to-diameter ratio L/D_s, 4.50; corrected data.

Figure 5. - Concluded. Comparison of hot- and cold-ejector performance for various length-to-diameter ratios. Diameter ratio D_s/D_p, 1.21; spacing S/D_p, 0.82.

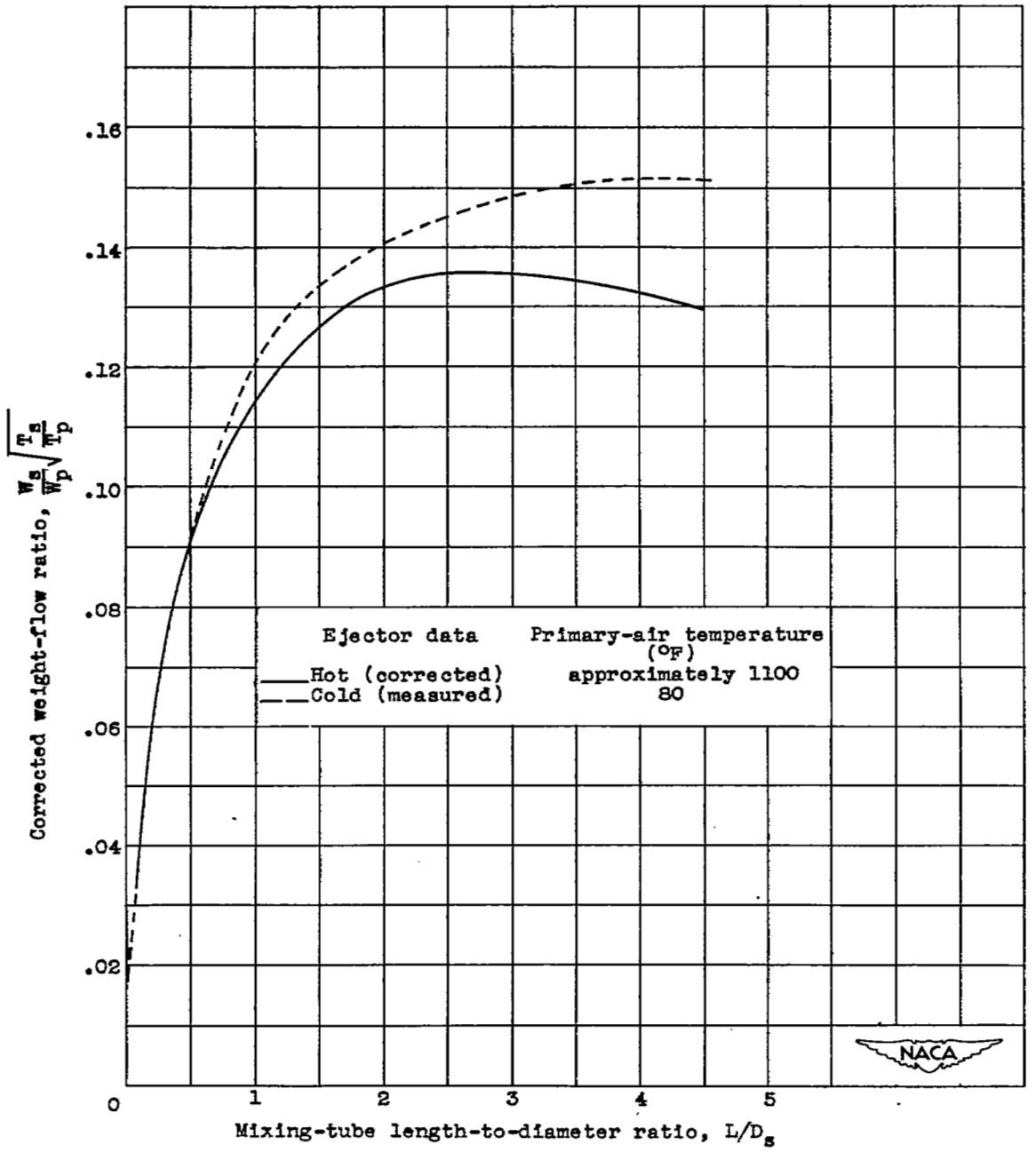

Figure 6. - Effect of mixing-tube length on the agreement between corrected hot-ejector data and cold-ejector data. Diameter ratio D_s/D_p, 1.21; spacing S/D_p, 0.82; primary pressure ratio $P_{p,1}/p_0$, 1.50; secondary pressure ratio $P_{s,1}/p_0$, 0.925.

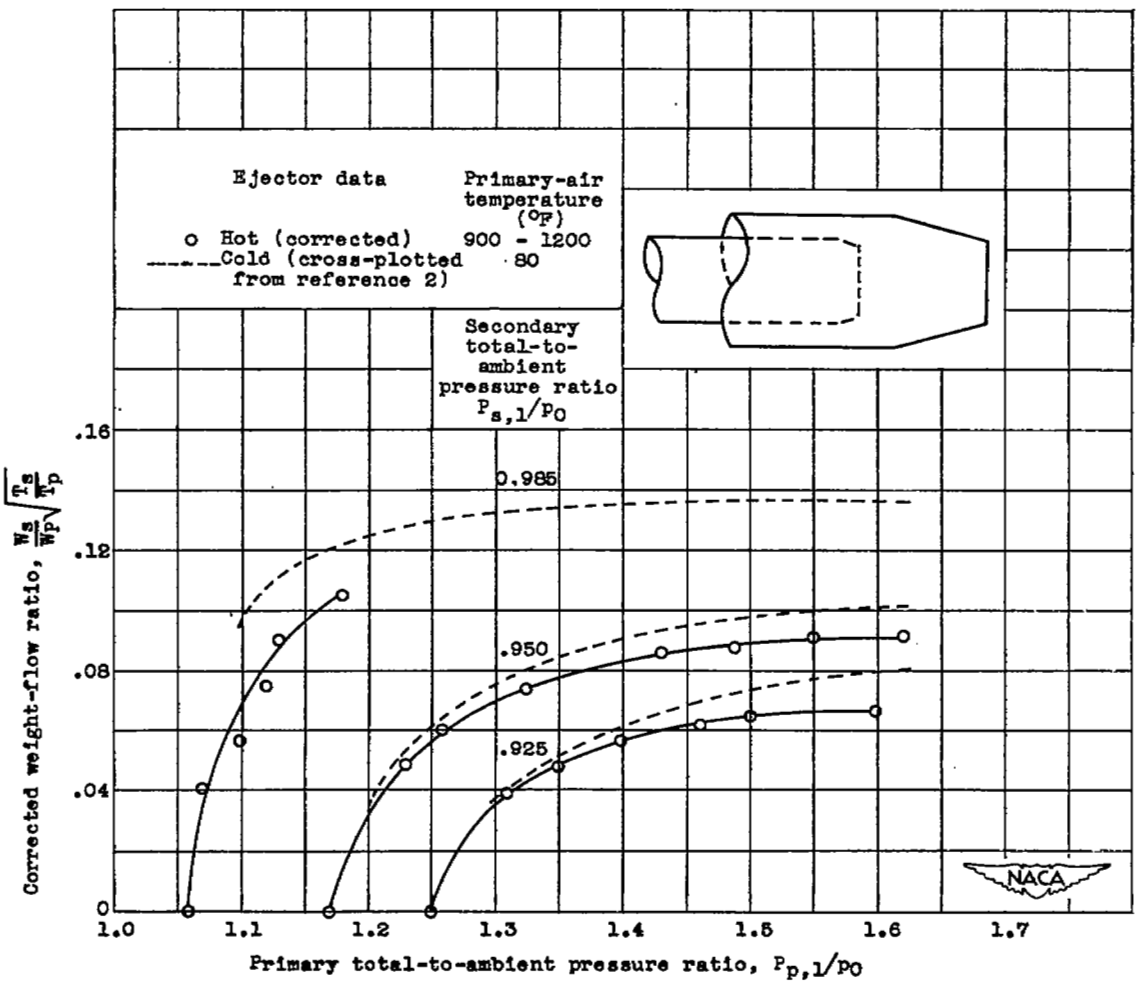

(a) Diameter ratio D_s/D_p, 1.21; spacing S/D_p, 1.64.

Figure 7. - Comparison of hot- and cold-ejector performance for two diameter ratios and spacings. Length-to-diameter ratio L/D_s, 0.

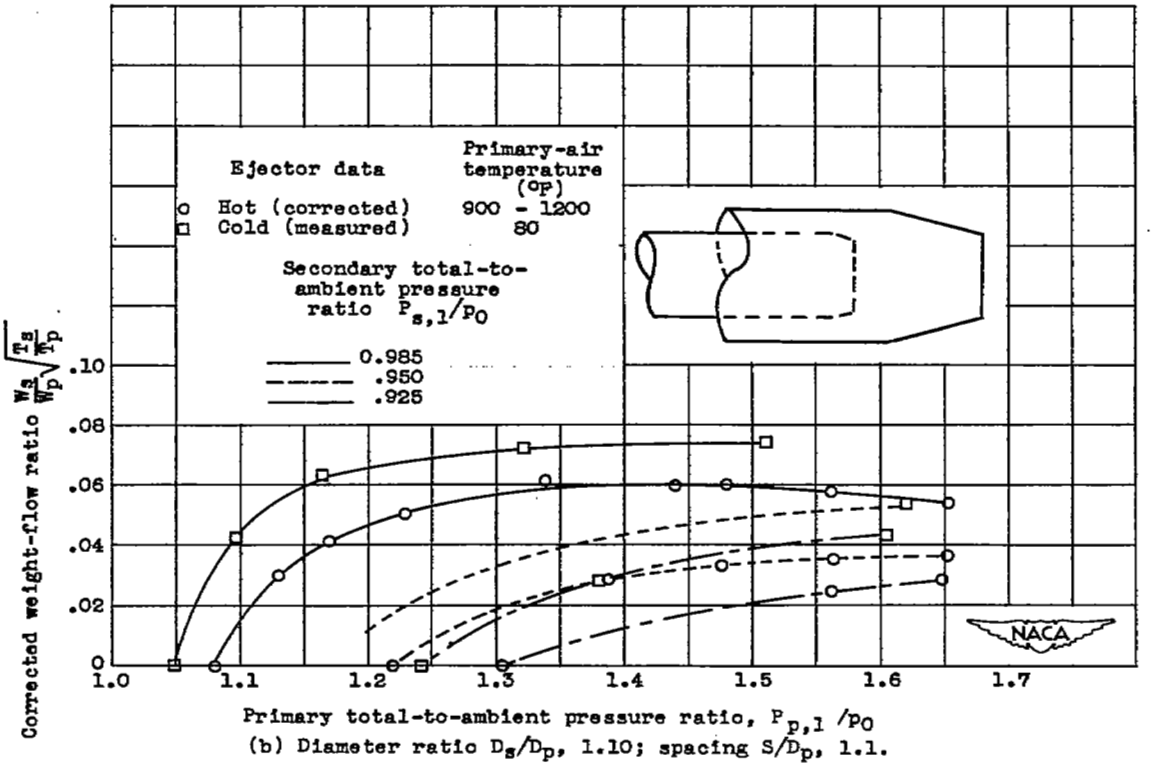

(b) Diameter ratio D_s/D_p, 1.10; spacing S/D_p, 1.1.

Figure 7. - Concluded. Comparison of hot- and cold-ejector performance for two diameter ratios and spacings. Length-to-diameter ratio L/D_s, 0.